Intensification of landfalling typhoons over the northwest Pacific since the late 1970s

Wei Mei[1,2*] and Shang-Ping Xie[1]

Intensity changes in landfalling typhoons are of great concern to East and Southeast Asian countries[1]. Regional changes in typhoon intensity, however, are poorly known owing to inconsistencies among different data sets[2–8]. Here, we apply cluster analysis to bias-corrected data and show that, over the past 37 years, typhoons that strike East and Southeast Asia have intensified by 12–15%, with the proportion of storms of categories 4 and 5 having doubled or even tripled. In contrast, typhoons that stay over the open ocean have experienced only modest changes. These regional changes are consistent between operational data sets. To identify the physical mechanisms, we decompose intensity changes into contributions from intensification rate and intensification duration. We find that the increased intensity of landfalling typhoons is due to strengthened intensification rates, which in turn are tied to locally enhanced ocean surface warming on the rim of East and Southeast Asia. The projected ocean surface warming pattern under increasing greenhouse gas forcing suggests that typhoons striking eastern mainland China, Taiwan, Korea and Japan will intensify further. Given disproportionate damages by intense typhoons[1], this represents a heightened threat to people and properties in the region.

Tropical cyclones (TCs) cause devastating losses of life and property, and have major social and economic impacts around the world[1]. Given that nearly all the damage is associated with TC landfalls, and that the population of coastal areas is growing and sea level is rising, detection, attribution and prediction of regional changes in TC activity (especially intensity and frequency) are among the top priorities of TC research[9,10]. For the northwest Pacific, where TCs are most active and threaten a large population of East and Southeast Asia, progress in studying regional changes in TC intensity has been hindered by a lack of consensus on intensity changes among different TC data sets[2–8]. Particularly, under debate are historical changes in the annual counts of category 4–5 typhoons: the Joint Typhoon Warming Center (JTWC) and the Japan Meteorological Agency (JMA) TC data—the two most widely used data sets in typhoon research—show contradictory trends for the period starting from 1977[2,3,6,7].

The discrepancies in the TC intensity estimated independently by the two operational agencies can be reconciled by considering changes in the JMA methodology (see Methods). The adjusted JMA and JTWC data sets consistently show that the annual number of category 4–5 typhoons has increased by more than two over the past 38 years (from less than five per year to around seven per year), and the correlation coefficient between the two time series rises from 0.09 to 0.87 after the adjustment (Fig. 1a). Strikingly, the proportion of these intense typhoons to all typhoons has more than doubled, and the annual mean typhoon lifetime peak intensity has increased by 14% ($\sim$7 m s^{-1})—a nearly 50% increase in instantaneous destructiveness[11]—during 1977–2014 (Fig. 1b,c), suggesting a substantial shift to higher typhoon intensity[8,11–14]. This is corroborated by the results from a coupled downscaling model (Supplementary Fig. 1). It remains to be determined whether the 38-year trend we identified here is part of low-frequency oscillations or secular climate change.

Around 50% of typhoons make landfall (Supplementary Table 1), and an increase in landfalling typhoon intensity would be of great concern for society. While previous studies have focused on basin-integrated intensity metrics[2–4,8,11,12,14–16], here we investigate regional characteristics of typhoon intensity change. We use cluster analysis to divide typhoons into four distinct regional groups, a method that proves successful in identifying patterns of northwest Pacific TC tracks[17,18]. To obtain robust features, we apply the cluster analysis jointly to both JTWC and adjusted JMA data sets (see Methods). Our results reveal that typhoon groups with the largest landfall rates show pronounced intensification, whereas changes in open-ocean typhoons are modest in comparison.

We find that four clusters are optimal to distinguish typhoons of different characteristics (for example, geographic locations of genesis and tracks) while retaining a large sample size in each cluster to study interannual and longer variations. Typhoon statistics in each group are given in Supplementary Table 1. Clusters 1 and 2 include more than 60% of typhoons over the entire basin with a high landfall rate ($\sim$85%). As detailed below, typhoons of these two clusters show the most pronounced increasing trends in intensity and intensification rate.

Figure 2 shows the tracks and temporal evolution of different intensity metrics of typhoons in Cluster 1, which constitute around 34% of the northwest Pacific typhoons (Supplementary Table 1). After forming east of the Philippines, typhoons in this group travel northwestwards-to-northwards, and roughly 75% of them make landfall over East Asia (north of $\sim$22° N; including eastern mainland China, Taiwan, Korean and Japan). The annual mean values of their lifetime peak intensity have risen by $\sim$8 m s^{-1} ($\sim$15%) during 1977–2013 (Fig. 2b), the largest increase among the four groups. Consistently, category 4–5 typhoons have increased by nearly four times in number (from less than one per year in the late 1970s to more than four per year in recent years; Supplementary Fig. 2a; see a discussion in Methods) and nearly tripled as a percentage of total typhoon counts (from $\sim$20% to $\sim$60%; Supplementary Fig. 3a).

Figure 3 shows the results for typhoons in Cluster 2, which make up nearly 30% of the typhoons basin wide (Supplementary Table 1). They form slightly westward relative to those in Cluster 1 and over the South China Sea, and move more directly towards the west-to-northwest, with 97% of them striking Southeast Asia (including the Philippines and Vietnam) and/or South China.

[1]Scripps Institution of Oceanography, University of California at San Diego, 9500 Gilman Drive MC 0206, La Jolla, California 92093-0206, USA.
[2]Department of Marine Sciences, University of North Carolina at Chapel Hill, 3202 Venable and Murray Halls, CB 3300, Chapel Hill, North Carolina 27599-3300, USA. *e-mail: wmei@email.unc.edu

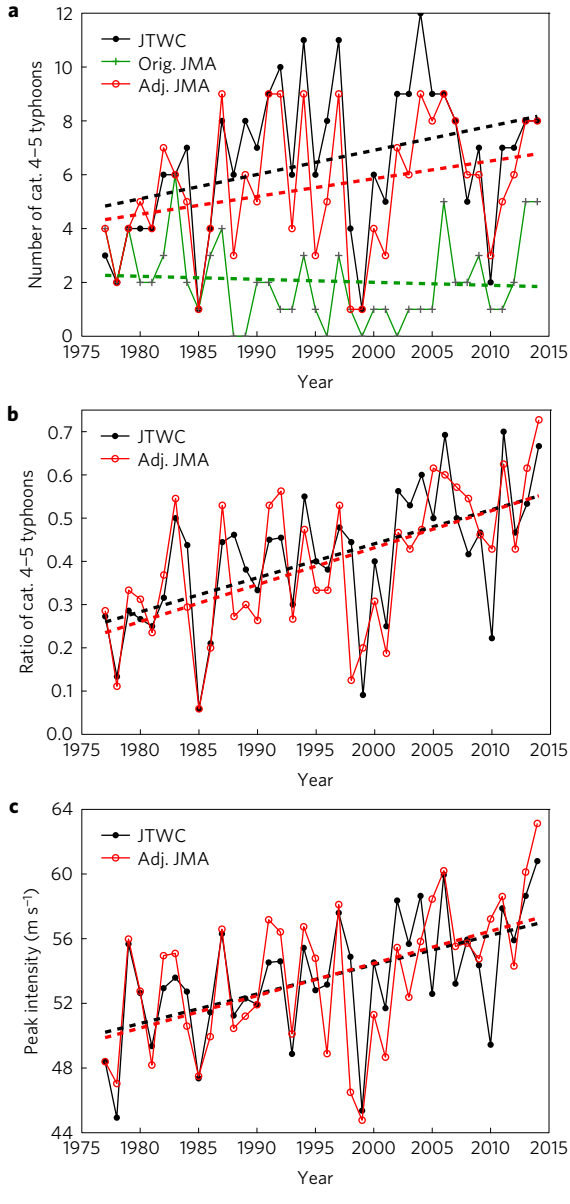

Figure 1 | Temporal evolution of various typhoon intensity metrics. **a**–**c**, Annual number of category (cat.) 4–5 typhoons (**a**), ratio of the annual number of category 4–5 typhoons to that of all typhoons (**b**), and annual mean typhoon lifetime peak intensity (**c**) in the northwest Pacific as a function of time from the JTWC data (black curve) and adjusted (adj.) JMA 1-min wind data (red curve; see Methods). Green curve in **a** shows results for the original (orig.) JMA 1-min wind data (obtained using JMA 10-min wind data and a conversion used in previous studies). Thick dashed lines in each panel show linear trends during 1977–2014.

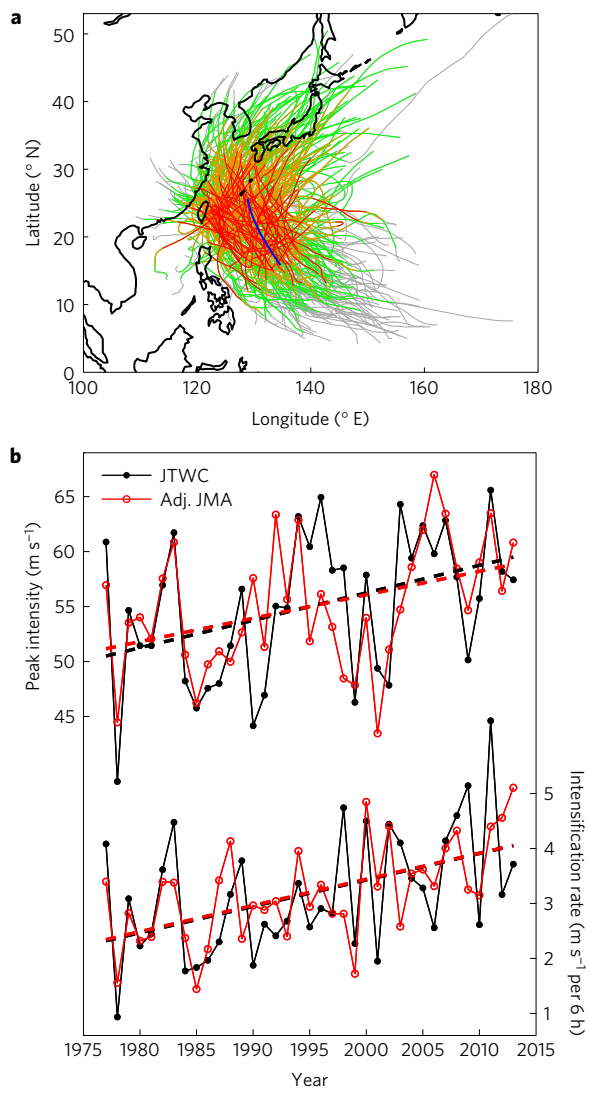

Figure 2 | Tracks and intensity evolution of typhoons in Cluster 1. **a**, Tracks of typhoons from the JTWC data (the JMA data show similar results). The colours show the intensity of tropical depression (grey), tropical storm (green), categories 1 and 2 (orange), and categories 3 to 5 (red). **b**, Annual mean typhoon lifetime peak intensity and annual mean typhoon intensification rate as a function of time from the JTWC (black curve) and adjusted JMA (red curve) data. Thick dashed lines show linear trends during 1977–2013.

Typhoons in this group on average have intensified by ~5 m s^{-1} (~12%) throughout the 37-year period (Fig. 3b). Category 4–5 typhoons have approximately doubled both in number (from slightly more than 0.5 per year to more than 1 per year; Supplementary Fig. 2b) and in proportion (from more than 10% to nearly 30%; Supplementary Fig. 3b).

Typhoons in Clusters 3 and 4 are generated farther east than those in the first two groups, and generally stay over the open ocean during their lifetime, with a much smaller chance of making landfall (Supplementary Figs 4 and 5 and Supplementary Table 1). They have also experienced some increases in their lifetime peak intensity and in the proportion reaching category 4–5 intensity over the study period, particularly for Cluster 4 (Supplementary Fig. 3c,d). But the very small sample size after year 2005 precludes a robust quantification (Supplementary Fig. 6c,d). It is worth noting that a decrease in the number of Cluster 4 typhoons and an increase in the number of Cluster 1 typhoons may have contributed to the observed poleward shift in the average latitude where typhoons reach their peak intensity[19].

To understand the cause of intensity change, we decompose the peak intensity into intensification rate and intensification duration, two metrics governed by distinct physical processes. While intensification duration variability is related to the El Niño–Southern Oscillation and the Pacific Decadal Oscillation[4,15,16,18,20], intensification rate change is tied to the sea surface temperature (SST) warming pattern (to be shown later). The intensification rate of Cluster 1 and 2 typhoons has increased by 1.5 m s^{-1} per 6 h—a more than 60% increase—during 1977–2013 (Figs 2b and 3b). Such a pronounced increase in intensification rate accounts for nearly all the strong increase in typhoon intensity in these two groups

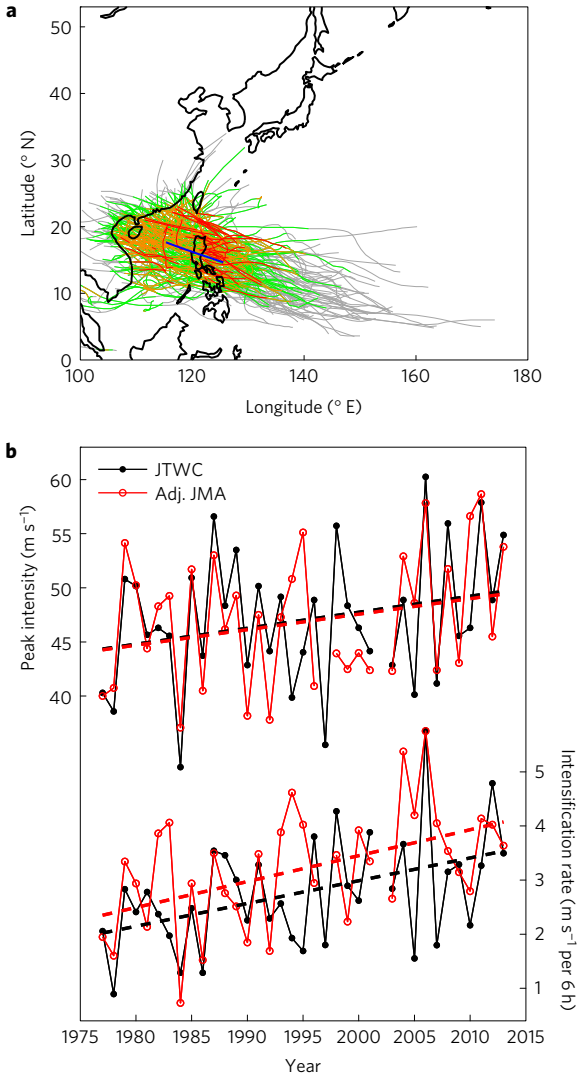

Figure 3 | Tracks and intensity evolution of typhoons in Cluster 2. a, Tracks of typhoons from the JTWC data (the JMA data show similar results). The colours show the intensity of tropical depression (grey), tropical storm (green), categories 1 and 2 (orange), and categories 3 to 5 (red). **b**, Annual mean typhoon lifetime peak intensity and annual mean typhoon intensification rate as a function of time from the JTWC (black curve) and adjusted JMA (red curve) data. Thick dashed lines show linear trends during 1977–2013.

(Figs 2b and 3b), with intensification duration contributing mainly to interannual-to-decadal variations (Supplementary Fig. 7a,b). By contrast, the intensification rate of Cluster 3 and 4 typhoons has experienced modest changes (Supplementary Figs 4b and 5b).

We have also examined an experimental data set obtained based on simplified analysis of satellite infrared images[21] (see Methods). In the experimental data set, Cluster 1 typhoons show a similar increasing trend of smaller magnitude in both lifetime peak intensity and intensification rate, but Cluster 2 typhoons exhibit no intensification trends. The reason for the discrepancies is unclear at this stage, but we note that operational best track data consider additional observations, including *in situ* measurements. While using similar data sources, JTWC and JMA conduct the Dvorak analysis independently. The agreement between the two operational data sets gives confidence in both. The experimental data set, on the other hand, shows systematic biases in the annual mean and probability density function of lifetime peak intensity during 1981–1987, when aircraft reconnaissance data were still available and incorporated into the operational data sets. The exact cause of these biases is beyond the scope of this study.

The above analyses based on the operational data sets suggest that changes in typhoon intensification rate display a marked spatial pattern: the changes are large and robust off East and Southeast Asia, whereas the changes are modest over the open ocean. To determine the physical factors for the spatial inhomogeneity in changes of typhoon intensification rate, we calculate the linear trend over the study period in various atmospheric and oceanic variables that affect typhoon development.

Figure 4a and Supplementary Fig. 9 show the results for potential intensity (a theoretical maximum intensity a TC can achieve for a given SST and atmospheric thermodynamic profile)[22,23], upper-ocean thermal stratification, vertical wind shear, and low-level vorticity. The most striking feature is the enhanced increase in potential intensity along the continental rim of East and Southeast Asia compared to the open ocean (Fig. 4a). This spatial pattern bears a strong resemblance to that of changes in typhoon intensification rate (see Supplementary Fig. 8 for the intensification region for each individual typhoon group), suggesting that potential intensity exerts a strong control on typhoon intensification, with higher potential intensity permitting more vigorous deep convection in favour of typhoon development[24].

Reduced upper-ocean thermal stratification (that is, temperature difference between sea surface and subsurface) over 20°–30° N, 120°–135° E and over the northern South China Sea (Supplementary Fig. 9a) may also contribute to an increasing typhoon intensification rate over these regions, by diminishing the negative feedback from typhoon-induced upper-ocean mixing[25,26]. The positive effect of weakened stratification over the tropical open ocean east of 130° E appears to be relatively minor in affecting local typhoon development; see Methods for a discussion of possible reasons. As for atmospheric dynamic variables (for example, vertical wind shear and low-level vorticity), their changes over the typhoon intensification regions are either modest or spatially sporadic, and do not represent robust contributions to typhoon intensification modulation (Supplementary Fig. 9b,c), except the possible effect of low-level vorticity noted in Methods.

The changes in potential intensity resemble the SST change pattern (Fig. 4a,b)[27,28], suggesting that local SST changes control typhoon intensification rate. To verify this SST effect, we further compute the correlation coefficient between interannual variations in the SST and the typhoon intensification rate of each individual group (Supplementary Fig. 11). Despite the small sample size and associated low signal-to-noise ratio, significant positive correlations exist between typhoon intensification rate and local SSTs for each cluster (Supplementary Fig. 11). (Calculations with global or Pacific tropical mean SST warming removed give consistent results with smaller values.) This suggests that the SST effect on typhoon intensification rate is present not only in the long-term trend but also in interannual variations. In addition, a rough estimate suggests that during the study period (that is, 1977–2013) the SST effect is twice as large as the stratification effect (see Methods); together they contribute to around 75% of the intensification rate increase. While SSTs have been suggested to regulate basin-integrated TC activity and the SST change pattern has been linked to TC frequency change[11,12,14,16,18,28–32], our results here indicate that the SST change pattern is an important predictor for regional typhoon intensity change. The SST change pattern itself may be related to changes in ocean currents and surface winds[33]. The observed SST change (including the spatial pattern) includes both natural and anthropogenic components[33,34]. Rigorous attribution of the observed change in typhoon intensification remains challenging, owing to a lack of long-term reliable data. Experiments with realistic high-resolution models may help separate anthropogenic trends from natural variability.

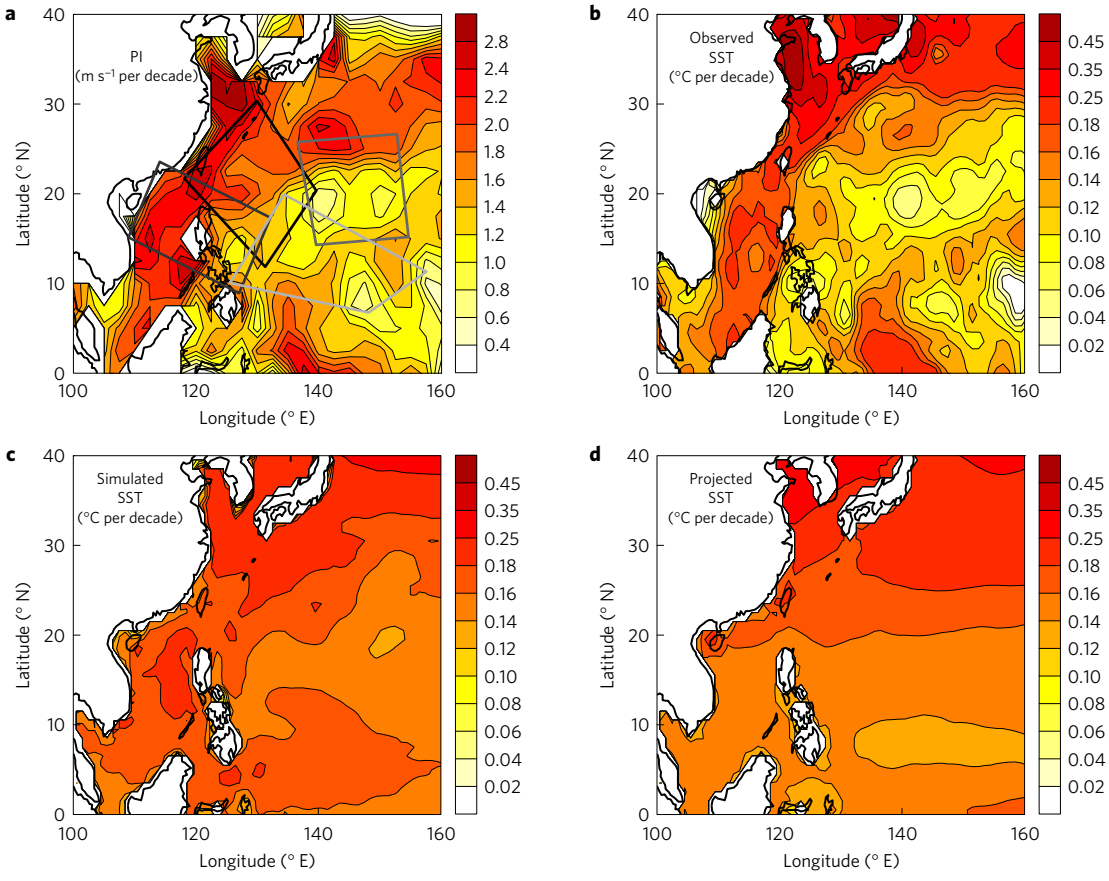

Figure 4 | Linear trends in potential intensity and SST. a–d, Spatial maps of linear trends in potential intensity (PI, m s^{-1} per decade) calculated using observed SSTs and atmospheric reanalysis data during 1977–2013 (**a**), observed SSTs (°C per decade) during 1977–2013 (**b**), simulated SSTs (°C per decade) during 1977–2013 (**c**) and projected SSTs (°C per decade) during 2006–2100 under the RCP 4.5 scenario by CMIP5 models (**d**). Model spreads, represented as standard deviation, of linear trends in projected SSTs are shown in Supplementary Fig. 13a. The four boxes in **a** that gradually fade from black to light grey show the main intensification regions of typhoons in the four groups (see Supplementary Fig. 8).

In summary, our analyses of TC data sets from independent operational agencies show that typhoons that make landfall have significantly intensified since the late 1970s owing to strengthened intensification rate. The increase in intensification rate is in turn due to enhanced SST warming in a band off the coast of East and Southeast Asia. Our results hence reveal the critical role of local SSTs in typhoon intensification, and suggest the importance of the SST change pattern for regional changes in typhoon intensity in a warming climate.

Climate models in the fifth phase of the Coupled Model Intercomparison Project (CMIP5) simulate the observed intensification of SST warming and increase of potential intensity on the continental rim of East and Southeast Asia, although the horizontal gradient is underestimated (Fig. 4c and Supplementary Fig. 12b). While quantitative attribution of the historical change awaits further studies, CMIP5 models project faster warming rates north of ~20° N under both representative concentration pathways (RCP) 4.5 and 8.5 scenarios (Fig. 4d and Supplementary Fig. 12a). This SST change pattern acts to strengthen potential intensity over the subtropical ocean (Supplementary Fig. 12c,d; see also ref. 35). This favours the intensification of Cluster 1 and 3 typhoons, heightening risks of typhoon damage to eastern mainland China, Taiwan, Korea, and Japan.

Methods

Methods, including statements of data availability and any associated accession codes and references, are available in the online version of this paper.

Received 26 April 2016; accepted 21 July 2016; published online 5 September 2016

References

1. Peduzzi, R. *et al*. Global trends in tropical cyclone risk. *Nat. Clim. Change* **2,** 289–294 (2012).
2. Wu, M.-C., Yeung, K.-H. & Chang, W.-L. Trends in western North Pacific tropical cyclone intensity. *EOS Trans. Am. Geophys. Union* **87,** 537–538 (2006).
3. Kamahori, H., Yamazaki, N., Mannoji, N. & Takahashi, K. Variability in intense tropical cyclone days in the western North Pacific. *SOLA* **2,** 104–107 (2006).
4. Chan, J. C. L. Decadal variations of intense typhoon occurrence in the western North Pacific. *Proc. R. Soc. A* **464,** 249–272 (2008).
5. Lander, M. A. A comparison of typhoon best-track data in the western North Pacific: irreconcilable differences. In *28th Conf. Hurricanes and Tropical Meteorology* (American Meteorological Society, 2008). https://ams.confex.com/ams/28Hurricanes/techprogram/paper_137395.htm
6. Song, J.-J., Wang, Y. & Wu, L. Trend discrepancies among three best track data sets of western North Pacific tropical cyclones. *J. Geophys. Res.* **115,** D12128 (2010).
7. Ren, F., Liang, J., Wu, G., Dong, W. & Yang, X. Reliability analysis of climate change of tropical cyclone activity over the western North Pacific. *J. Clim.* **24,** 5887–5898 (2011).
8. Kang, N.-Y. & Elsner, J. B. Consensus on climate trends in the western North Pacific tropical cyclones. *J. Clim.* **25,** 7564–7573 (2012).
9. Knutson, T. R. *et al*. Tropical cyclones and climate change. *Nat. Geosci.* **3,** 157–163 (2010).
10. Walsh, K. J. E. *et al*. Hurricanes and climate: the US CLIVAR Working Group on hurricanes. *Bull. Am. Meteorol. Soc.* **96,** 997–1017 (2015).
11. Emanuel, K. A. Increasing destructiveness of tropical cyclones over the past 30 years. *Nature* **436,** 686–688 (2005).

12. Webster, P. J., Holland, G. J., Curry, J. A. & Chang, H.-R. Changes in tropical cyclone number, duration, and intensity in a warming environment. *Science* **309,** 1844–1846 (2005).
13. Elsner, J. B., Kossin, J. P. & Jagger, T. H. The increasing intensity of the strongest tropical cyclones. *Nature* **455,** 92–95 (2008).
14. Holland, G. J. & Bruyère, C. L. Recent intense hurricane response to global climate change. *Clim. Dynam.* **42,** 617–627 (2014).
15. Chan, J. C. L. & Liu, K. S. Global warming and western North Pacific typhoon activity from an observational perspective. *J. Clim.* **17,** 4590–4602 (2004).
16. Mei, W., Xie, S.-P., Primeau, F., McWilliams, J. C. & Pasquero, C. Northwestern Pacific typhoon intensity controlled by changes in ocean temperatures. *Sci. Adv.* **1,** e1500014 (2015).
17. Camargo, S. J., Robertson, A. W., Gaffney, S. J., Smyth, P. & Ghil, M. Cluster analysis of typhoon tracks. Part I: general properties. *J. Clim.* **20,** 3635–3653 (2007).
18. Camargo, S. J., Robertson, A. W., Gaffney, S. J., Smyth, P. & Ghil, M. Cluster analysis of typhoon tracks. Part II: large-scale circulation and ENSO. *J. Clim.* **20,** 3654–3676 (2007).
19. Kossin, J. P., Emanuel, K. A. & Camargo, S. J. Past and projected changes in western North Pacific tropical cyclone exposure. *J. Clim.* http://dx.doi.org/10.1175/JCLI-D-16-0076.1 (2016).
20. Kim, H.-M., Webster, P. J. & Curry, J. A. Modulation of North Pacific tropical cyclone activity by three phases of ENSO. *J. Clim.* **24,** 1839–1849 (2011).
21. Kossin, J. P., Olander, T. L. & Knapp, K. R. Trend analysis with a new global record of tropical cyclone intensity. *J. Clim.* **26,** 9960–9976 (2013).
22. Emanuel, K. A. The maximum intensity of hurricanes. *J. Atmos. Sci.* **45,** 1143–1155 (1988).
23. Holland, G. J. The maximum potential intensity of tropical cyclones. *J. Atmos. Sci.* **54,** 2519–2541 (1997).
24. Knaff, J. A., Sampson, C. R. & DeMaria, M. An operational statistical typhoon intensity prediction scheme for the western North Pacific. *Weather Forecast.* **20,** 688–699 (2005).
25. Emanuel, K. Thermodynamic control of hurricane intensity. *Nature* **401,** 665–669 (1999).
26. Lin, I.-I. *et al*. An ocean coupling potential intensity index for tropical cyclones. *Geophys. Res. Lett.* **40,** 1878–1882 (2013).
27. Ramsay, H. A. & Sobel, A. H. Effects of relative and absolute sea surface temperature on tropical cyclone potential intensity using a single-column model. *J. Clim.* **24,** 183–193 (2011).
28. Korty, R. L., Camargo, S. J. & Galewsky, J. Tropical cyclone genesis factors in simulations of the Last Glacial Maximum. *J. Clim.* **25,** 4348–4365 (2012).
29. Sriver, R. & Huber, M. Low frequency variability in globally integrated tropical cyclone power dissipation. *Geophys. Res. Lett.* **33,** L11705 (2006).
30. Vecchi, G. A. & Soden, B. J. Effect of remote sea surface temperature change on tropical cyclone potential intensity. *Nature* **450,** 1066–1070 (2007).
31. Murakami, H., Wang, B. & Kitoh, A. Future change of western North Pacific typhoons: projections by a 20-km-mesh global atmospheric model. *J. Clim.* **24,** 1154–1169 (2011).
32. Zhao, M. & Held, I. M. TC-permitting GCM simulations of hurricane frequency response to sea surface temperature anomalies projected for the late-twenty-first century. *J. Clim.* **25,** 2995–3009 (2012).
33. Wu, L.-X. *et al*. Enhanced warming over the global western boundary currents. *Nat. Clim. Change* **2,** 161–166 (2012).
34. Jones, G. S., Stott, P. A. & Christidis, N. Attribution of observed historial near-surface temperature variations to anthropogenic and natural causes using CMIP5 simulations. *J. Geophys. Res. Atmos.* **118,** 4001–4024 (2013).
35. Camargo, S. J. Global and regional aspects of tropical cyclone activity in the CMIP5 models. *J. Clim.* **26,** 9880–9902 (2013).

Acknowledgements

We are very grateful to K. Emanuel for providing synthetic tropical cyclones simulated using a coupled downscaling tropical cyclone model. We also acknowledge the World Climate Research Program's Working Group on Coupled Modeling, which is responsible for CMIP, and we thank the climate modelling groups (listed in Supplementary Table 2) for producing and making available their model output. For CMIP, the US Department of Energy's Program for Climate Model Diagnosis and Intercomparison provides coordinating support and led development of software infrastructure in partnership with the Global Organization for Earth System Science Portals. This research was supported by NSF (1305719 and 1249145).

Author contributions

W.M. conceived and designed the study, performed the analyses, and wrote the paper. S.-P.X. contributed to the development of the idea and the writing of the paper.

Additional information

Supplementary information is available in the online version of the paper. Reprints and permissions information is available online at www.nature.com/reprints. Correspondence and requests for materials should be addressed to W.M.

Competing financial interests

The authors declare no competing financial interests.

Methods

Operational JTWC and JMA data sets. The tropical cyclone (TC) data over the northwest Pacific are from the Joint Typhoon Warning Center (JTWC) best track data set[36] and the Japan Meteorological Agency (JMA) best track data set, both of which provide TC location and intensity (measured by maximum sustained surface wind speed) at 6-h intervals. JTWC and JMA estimate the tracks and intensity of TCs independently, although they may use similar data sources (for example, satellite images) and techniques (for example, the Dvorak technique). Because JMA has provided wind speed measurements since 1977, we focus our study over the period of 1977–2014. Because the TC data for year 2014 were not available from JTWC at the time of analysis, the joint analysis of TC tracks covers only the period of 1977–2013. But analyses of basin-wide metrics (such as TC counts and lifetime peak intensity; Fig. 1) include year 2014, with the data of this year for JTWC being supplemented with the data from Unisys Weather (http://weather.unisys.com/hurricane/w_pacific/2014/index.php). We focus on TCs that reach typhoon intensity ($\sim$33 m s^{-1}) because of their dramatic influence in many aspects. In total, there are nearly 600 typhoons used in this study.

Adjusted JMA data set. JTWC and JMA provide maximum sustained wind speeds averaged over different time periods: 1 min for JTWC and 10 min for JMA. Here to be consistent with the JTWC data and to follow the Saffir–Simpson hurricane wind scale, we convert the JMA data from 10-min mean values to 1-min mean values. The conversion differs for the periods before and after the late 1980s, because JMA employed different methodologies in estimating the 10-min sustained wind speed[37–39]. Before 1987, JMA estimated 1-min sustained wind speeds first and then converted them to 10-min values based on a linear relationship. After 1987, JMA estimated 10-min sustained wind speed directly using the Koba table[40]. Accordingly, our conversion of the JMA data to 1-min mean values differs before and after 1987: the data before 1987 are divided by 0.88 (ref. 41), whereas the data after are first converted back to Dvorak current intensity number using the Koba table, which is then used to calculate 1-min mean values using the Dvorak table[42]. It is worth mentioning that the conversion used in previous studies appears not to have considered the changes in methodologies by JMA and that the JMA data are divided by a constant (for example, 0.88) over the entire period, producing results very different from those based on the new conversion (for example, see the green curve in Fig. 1a). We refer to the 1-min wind data obtained using the conversion in previous studies as the original JMA 1-min wind data and the data obtained using the new conversion in this study as the adjusted JMA 1-min wind data.

Because wind estimates in the adjusted JMA data are generally smaller than those in the JTWC data, particularly for intense typhoons (the mean lifetime peak intensity of category 4–5 typhoons is 67.95 and 64.88 m s^{-1} for the JTWC and adjusted JMA data, respectively), we reduce the threshold value of category 4 intensity slightly for the adjusted JMA data from 58.5 to 56 m s^{-1}, although keeping the value of 58.5 m s^{-1} produces similar results. The definition of typhoons is the same for the JTWC and adjusted JMA data. Despite the subjective nature of satellite imagery analyses and differences in how *in situ* measurements are incorporated into intensity estimates between agencies, the JTWC and adjusted JMA data show consistent trends in both basin and regional typhoon intensity metrics (for example, Figs 1–3), suggesting the robustness of our results. We further examined the simulations of a coupled downscaling TC model developed by Emanuel[43,44], and found a positive trend of similar magnitude in the annual mean typhoon lifetime peak intensity ($\sim$1.8 m s^{-1} per decade; Supplementary Fig. 1). In addition, we note that the positive trend in typhoon intensity in both the JTWC and JMA data is also in line with recent modelling studies (for example, ref. 45) and with the analyses using independent meteorological and oceanographic data sets[4].

The Kossin *et al.* data set. A new experimental TC data set based solely on satellite infrared imagery analysis has been recently developed[21] (hereafter the K13 data set). We have compared the K13 and JTWC data sets during 1981–1987, when aircraft reconnaissance observations were available, and used in the JTWC data set. Although the K13 data agree with the JTWC data on interannual timescales in terms of the annual mean typhoon lifetime peak intensity, obvious differences are identified: in the K13 data set, the probability density function of TC lifetime peak intensity shows a spurious dip for intensity between 40 and 50 m s^{-1}; also the peak intensity of typhoons is systemically biased high by 4 m s^{-1}. In addition, we evaluated the data sets for five additional northwest Pacific typhoons after 1987 for which *in situ* measurements were available. The RMS error of the K13 data is 9.5 m s^{-1}, three times that of the JTWC data (3.1 m s^{-1}).

The following technical issues may cause the above discrepancies. First, the K13 algorithm is basically a simplified Dvorak method and uses only infrared satellite imagery. The intensity estimates moderately correlate with aircraft reconnaissance-measured intensity[46]. Second, the K13 algorithm was trained primarily over the North Atlantic, and may not be applied to the northwest Pacific. Indeed, regional adjustments are required in estimating TC intensity with the Dvorak technique[47].

In contrast, operational centres (for example, JTWC and JMA) use the Dvorak method, which takes multi-sensor remote sensing and, in addition, consider *in situ* observations (for example, aircraft dropsondes, ships and buoys) to estimate TC intensity. The operational best track data are considered to be more accurate, as corroborated by mutual consistency between the data sets of JTWC and JMA that conduct the Dvorak analysis independently, and by independent high-resolution downscaling model results.

In light of the above comparisons, we chose not to use the K13 data set. The philosophy of creating a homogeneous data set is very appealing, and such a data set of improved accuracy would be highly valuable.

Calculations of typhoon metrics. For each typhoon location, the intensification rate is computed by central differencing the maximum 1-min sustained surface wind speed at a 12-h interval. Translation speed is calculated by dividing the sum of the respective distance the typhoon moves six hours before and six hours after reaching the current position by the total time interval (that is, 12 h), using the positions reported in the best track data. Then, for each individual typhoon, we can get a mean value of intensification rate and mean translation speed by simply averaging the values at all locations during its intensification period (that is, from the TC reaching typhoon intensity for the first time until its lifetime peak intensity), and the duration of intensification is accordingly defined as the length of this intensification period. Since here we are more interested in the variation in the annual mean, the mean intensification rate, mean translation speed, and duration of intensification of each typhoon are then used to calculate the annual mean values using all typhoons during that year for each individual cluster. These calculations are performed separately for the JTWC and JMA data.

Analysis of large-scale atmospheric and oceanic conditions. Atmospheric variables including zonal and meridional winds, air temperature, pressure, and relative humidity from NCEP/NCAR Reanalysis 1 (ref. 48), sea surface temperatures (SSTs) from the Hadley Centre SST data set[49], and ocean temperature data from the World Ocean Database 2013 (ref. 50) are used to identify the mechanisms underlying the variability in annual mean typhoon intensification rate. The first three data sets have a monthly temporal resolution, and the last one has a temporal resolution of three months (that is, January–March, April–June, July–September, and October–December for each year). We use the data during July–November to represent the typical atmospheric and oceanic conditions during the typhoon peak season[11]. We tested the sensitivity of the results using data between July and October and reached the same conclusions. Consistent results can be obtained using other reanalysis data sets: similar spatial pattern of potential intensity trends are shown in other studies[51–53] using the ERA-interim and MERRA reanalysis data sets, albeit with differences in the amplitude of the trends.

A joint cluster analysis of typhoon tracks. A clustering technique developed by ref. 54 and widely used in previous studies[17,18] is employed to group typhoons into different clusters based on the geographic locations of their genesis and the subsequent tracks. The description of this technique parallels that of ref. 17, as follows: our curve clustering method is based on the finite mixture model, which represents a data distribution as a convex linear combination of component density functions. A key feature of the mixture model is its ability to model highly non-Gaussian (and possibly multimodal) densities. Regression mixture models extend the standard mixture modelling framework by replacing the marginal component densities with conditional density components. The component densities [in this study] model a cyclone's longitudinal and latitudinal positions versus time using quadratic polynomial regression functions. The latitude and longitude positions are treated as conditionally independent given the model, and thus the complete function for a cyclone track is the product of these two. Each trajectory (that is, each cyclone track) is assumed to be generated by one of K [$K = 4$ in this study] different regression models, each having its own shape parameters. The clustering problem is to learn the parameters of all K models given the TC tracks, and then infer which of the K models are most likely to have generated that track given the model. In other words, the assigned cluster has the highest posterior probability given the track.

Only tracks with the storm intensity being tropical storm or above are considered. Because the tracks from the best track data sets by different agencies differ (though not that much), even for a specific storm (that is, having a same name around the same time)[39], we apply the cluster technique to tracks from both the JTWC and JMA data sets simultaneously to obtain robust conclusions (that is, inclusion of the tracks from both the JTWC and JMA data in the same analysis). We note that the clustering method is more objective than a method in which typhoons are first divided into different groups based on whether they make landfall, although the latter method produces similar results.

A note on changes in typhoon number in Cluster 1. Part of the increase in the absolute number of typhoons and category 4–5 typhoons may be due to a geographical shift in the number of typhoons between Cluster 1 and Cluster 4

(see Supplementary Fig. 6a,d), which may be modulated by climate variability, such as the El Niño–Southern Oscillation[4,15,18,20,55]. (The geographical shift in the number of typhoons among clusters may change the average latitude where typhoons reach their peak intensity and change the pattern of typhoon track density[19,56].) This, however, does not affect the robustness of the finding that the percentage of typhoons in Cluster 1 developing to category 4–5 intensity has increased with time (Supplementary Fig. 3a), which is independent of the changes in the absolute number of typhoons in this group.

A note on changes in typhoon intensity of Cluster 4. The rising trend in typhoon intensity of Cluster 4 before 2005 is mostly attributed to an increase in typhoon intensification duration (Supplementary Figs 5b and 7d), which is in turn associated with the El Niño–Southern Oscillation and the Pacific Decadal Oscillation[4,15,16,18,20,55]; the high intensity in more recent years appears to be primarily due to changes in intensification rate (Supplementary Fig. 5b).

Possible reasons for the minor effect of weakened stratification over tropical open ocean east of 130° E on local typhoon development. First, in this area the climatological stratification is relatively weak (Supplementary Fig. 10a) and typhoons are moving relatively fast (Supplementary Table 1). Accordingly, TC-induced SST cooling is expected to be small (Supplementary Fig. 10b) with a consequent weak influence on typhoon development[57–59]. This, together with the nonlinear dependence of TC intensification rate on SST cooling[57,58], leads to a weak sensitivity of typhoon intensification to changes in stratification. Second, reduced low-level vorticity east of the Philippines (Supplementary Fig. 9c) may have cancelled the weak positive effect of reduced upper-ocean thermal stratification.

A rough estimate of the SST and ocean thermal stratification effect on typhoon intensification rate. Over the intensification regions of Cluster 1 and 2 typhoons, the SST warming rate is around 0.2 °C per decade and the weakening rate of ocean thermal stratification is around 0.1 °C per decade. Their respective effect on typhoon intensification rate is approximately +0.2 and +0.1 m s^{-1} per 6 h per decade[16], which is ~50% and 25% of the observed increasing rate of typhoon intensification rate (0.4 m s^{-1} per 6 h per decade or 1.5 m s^{-1} per 6 h between 1977 and 2013).

Code availability. The code and scripts used to analyse the data and to generate the plots in this paper are available from the corresponding author on request.

Data availability. Tropical cyclone best track data are provided by the Joint Typhoon Warning Center (http://www.usno.navy.mil/NOOC/nmfc-ph/RSS/jtwc/best_tracks/wpindex.php) and the Japan Meteorological Agency (http://www.jma.go.jp/jma/jma-eng/jma-center/rsmc-hp-pub-eg/trackarchives.html). NCEP/NCAR Reanalysis 1 is provided by the USA National Oceanographic and Atmospheric Administration's (NOAA) Earth System Research Laboratory (http://www.esrl.noaa.gov/psd/data/gridded/data.ncep.reanalysis.html). SSTs are provided by the Met Office Hadley Centre (HadISST; http://www.metoffice.gov.uk/hadobs/hadisst). Ocean temperatures are provided by the NOAA's National Centers for Environmental Information (World Ocean Database 2013; https://www.nodc.noaa.gov/OC5/WOD13). CMIP5 output is from http://cmip-pcmdi.llnl.gov/cmip5/data_portal.html.

References

36. Chu, J.-H., Sampson, C. R., Levine, A. S. & Fukada, E. *The Joint Typhoon Warning Center Tropical Cyclone Best-Tracks, 1945–2000* NRL/MR/7540-02-16 (Naval Research Laboratory, 2002).
37. National Typhoon Center, Japan Meteorological Agency *Operational Tropical Cyclone Analysis by the Japan Meteorological Agency* Report (World Meteorological Organization, 2011); https://www.wmo.int/pages/prog/www/tcp/documents/JMAoperationalTCanalysis.pdf
38. Kishimoto, K. *JMA Best Track Data* Presentation (NOAA's National Climatic Data Center, 2011); ftp://eclipse.ncdc.noaa.gov/san1/ibtracs/workshop/SecondWorkshop/12-Tuesday/April-12-1340-JMA%20best%20track-Kishimoto.pptx
39. Lowry, M. R. *Developing a Unified Superset in Quantifying Ambiguities Among Tropical Cyclone Best Track Data for the Western North Pacific* Diploma thesis, Paper 1026, Florida State Univ. (2008).
40. Koba, H., Hagiwara, T., Osano, S. & Akashi, S. Relationship between the CI-number and central pressure and maximum wind speed in typhoons. *J. Meteor. Res.* [*in Japanese*] **42,** 59–67 (1990).
41. Kruk, M. C., Knapp, K. R. & Levinson, D. H. A technique for combining global tropical cyclone best track data. *J. Atmos. Oceanic Technol.* **27,** 680–692 (2010).
42. Dvorak, V. F. *Tropical Cyclone Intensity Analysis Using Satellite Data, Tech. Rep. 11* 45 (NOAA, 1984).
43. Emanuel, K. Climate and tropical cyclone activity: a new model downscaling approach. *J. Clim.* **19,** 4797–4802 (2006).
44. Emanuel, K., Sundararajan, R. & Williams, J. Hurricanes and global warming: results from downscaling IPCC AR4 simulations. *Bull. Am. Meteorol. Soc.* **89,** 347–367 (2008).
45. Wu, L.-G. & Zhao, H. Dynamically derived tropical cyclone intensity changes over the western North Pacific. *J. Clim.* **25,** 89–98 (2012).
46. Olander, T. L. & Velden, C. S. The Advanced Dvorak technique: continued development of an objective scheme to estimate tropical cyclone intensity using geostationary infrared satellite imagery. *Weather Forecast.* **22,** 287–298 (2007).
47. Velden, C. *et al*. The Dvorak tropical cyclone intensity estimation technique: a satellite-based method that has endured for over 30 years. *Bull. Am. Meteorol. Soc.* **87,** 1195–1210 (2006).
48. Kalnay, E. *et al*. The NCEP/NCAR 40-Year Reanalysis Project. *Bull. Am. Meteorol. Soc.* **77,** 437–471 (1996).
49. Rayner, N. A. *et al*. Global analyses of sea surface temperature, sea ice, and night marine air temperature since the late nineteenth century. *J. Geophys. Res.* **108(D14),** 4407 (2003).
50. Boyer, T. P. *et al*. World Ocean Database 2013, NOAA Atlas NESDIS 72 (ed. Levitus, S.; technical ed. Mishonov, A.) 209 (NOAA, 2013).
51. Vecchi, G. A., Fueglistaler, S., Held, I. M., Knutson, T. R. & Zhao, M. Impacts of atmospheric temperature trends on tropical cyclone activity. *J. Clim.* **26,** 3877–3891 (2013).
52. Kossin, J. P. Validating atmospheric reanalysis data using tropical cyclones as thermometer. *Bull. Am. Meteorol. Soc.* **96,** 1089–1096 (2015).
53. Choi, Y., Ha, K.-J., Ho, C.-H. & Chung, C. E. Interdecadal change in typhoon genesis condition over the western North Pacific. *Clim. Dyn.* **45,** 3243–3255 (2015).
54. Gaffney, S. J., Robertson, A. W., Smyth, P., Camargo, S. J. & Ghil, M. Probabilistic clustering of extratropical cyclones using regression mixture models. *Clim. Dyn.* **29,** 423–440 (2007).
55. Camargo, S. J. & Sobel, A. H. Western North Pacific tropical cyclone intensity and ENSO. *J. Clim.* **18,** 2996–3006 (2005).
56. Kossin, J. P., Emanuel, K. A. & Vecchi, G. A. The poleward migration of the location of tropical cyclone maximum intensity. *Nature* **509,** 349–352 (2014).
57. Mei, W., Pasquero, C. & Primeau, F. The effect of translation speed upon the intensity of tropical cyclones over the tropical ocean. *Geophys. Res. Lett.* **39,** L07801 (2012).
58. Vincent, E. M., Emanuel, K. A., Lengaigne, M., Vialard, J. & Madec, G. Influence of upper ocean stratification interannual variability on tropical cyclones. *J. Adv. Model. Earth Syst.* **6,** 680–699 (2014).
59. Mei, W., Lien, C.-C., Lin, I.-I. & Xie, S.-P. Tropical cyclone-induced ocean response: a comparative study of the South China Sea and tropical northwest Pacific. *J. Clim.* **28,** 5952–5968 (2015).